

Impurity effect on the Fröhlich conductivity in NbSe₃

J. W. Brill,* N. P. Ong, J. C. Eckert, and J. W. Savage

Department of Physics, University of Southern California, Los Angeles, California 90007

S. K. Khanna and R. B. Somoano

Jet Propulsion Laboratory, California Institute of Technology, Pasadena, California 91103

(Received 16 May 1980)

The effect of Ta and Ti impurities on the anomalous transport properties (non-Ohmic dc conductivity and excess microwave absorption) of NbSe₃ has been studied. Data from 22 samples show that the characteristic field E_0 and the threshold field E_T are very sensitive to doping. Both E_0 and E_T obey a c^2 behavior where c is the Ta concentration. The anomalous microwave response is also suppressed by the presence of impurities. As in the dc case Ti is more effective than Ta in suppressing the anomalous behavior. These impurity studies lend strong support to the Fröhlich model in which the dc non-Ohmicity is ascribed to a sliding mode of the charge-density-wave condensate and the excess microwave absorption is ascribed to resonant oscillations of the condensate about pinning centers. The presence of impurities suppresses both the sliding and oscillatory modes. We also briefly describe the effect of the dynamic response of the massive condensate to very short pulses and its effect on non-Ohmic measurements.

I. INTRODUCTION

The non-Ohmicity in the conductivity¹ and the excess microwave absorption² observed in the compound NbSe₃ are dramatic manifestations of collective behavior in the charge-density-wave (CDW) state. In the purest samples studied deviations from Ohm's law appear when the dc electric field at 50 K exceeds 10 mV/cm. The microwave conductivity in the CDW state is also observed to be very different from the dc (Ohmic) value.

Although no single model has succeeded in explaining all the experimental data in the nonlinear regime the Fröhlich sliding-mode³⁻⁵ model is currently favored by most of the reported experiments. Strong support for sliding conductivity is provided by the x-ray scattering data⁶ and the impurity studies.⁷ In the latter the characteristic electric field E_0 has been varied from 20 to 2000 mV/cm by light doping with Ta. Preliminary results⁷ showed that E_0 varies as the square of the impurity concentration c in agreement with a calculation by Lee and Rice⁵ (LR) based on the Fröhlich model. Here we present a detailed report on these measurements as well as discussions on the field dependence of the non-Ohmic conductivity. Recently Fleming and Grimes⁸ (FG) proposed that a better fit to the non-Ohmic conductivity is obtained by introducing a third parameter E_T (the threshold field) into the Zener-type expression originally suggested by Monceau *et al.*¹ and Ong and Monceau² (OM). A reanalysis of our data and more extensive measurements confirm the existence of E_T . We show that this does not alter the conclusion in Ref. 7, i.e., below the second tran-

sition E_0 varies as c^2 . We also find on the basis of fewer data points that E_T also varies as c^2 . For completeness we also report on the microwave absorption data, augmented by some recent results.

In Sec. IV we discuss the "goodness of fit" of the modified Zener-type expression and also comment on recent measurements of the non-Ohmicity by Gill⁹ and by Richards and Monceau¹⁰ (RM). In Sec. V we briefly review the comparison between experiment and theoretical predictions of various models. Section V also discusses a newly observed physical effect¹¹ (tentatively identified with the inertial dynamic response of the condensate) which has a direct bearing on the non-Ohmic pulsed measurements.

II. EXPERIMENTAL DETAILS

Samples of NbSe₃ were grown as described by Meerschaut and Rouxel¹² by heating stoichiometric proportions of Nb and Se in a quartz tube (1-inch diameter) for 3 weeks at 720 °C. For the doped compounds Nb_{1-c}Ta_cSe₃ or Nb_{1-c}Ti_cSe₃, where c varies from 100 to 1900 ppm, the alloy Nb_{1-c}Ta_c or Nb_{1-c}Ti_c was first made by melting together "pure" Nb (180 ppm Ta content) and Ta or Ti followed by successive cycles of cutting and remelting. The desired value of c was then obtained by introducing nominally pure Nb followed by further cycles of remelting. Then the samples were grown as above. No attempt was made to determine the homogeneity of the crystals obtained from a batch or the value of c in a given crystal. Instead we have characterized the purity of the sam-

ples by measuring the RRR (ratio of the room-temperature resistance to the resistance at 4 K) hereafter called \mathcal{R} . In general we found that \mathcal{R} correlates roughly with the nominal value of c in a given batch (Fig. 1 inset). Crystals obtained from the same tube will have values which cluster around a mean with typically 20% dispersion, and we have assumed⁷ that \mathcal{R}^{-1} is linear in the actual impurity concentration of a crystal.

The reasonableness of this assumption follows from the substantial fraction of normal carriers remaining uncondensed at 4 K (Ref. 13) and their high mobility; electron mobilities approaching $250\,000\text{ cm}^2/\text{V s}$ at 4 K have been indicated by galvanomagnetic studies¹³ and large Shubnikov-de Haas (SdH) oscillations.¹⁴ The large fraction of uncondensed carriers suggests that \mathcal{R} would be proportional to an average low-temperature mobility. We have checked this by measuring the trans-

verse magnetoresistance, as described elsewhere,¹⁵ at 4.2 K for five Ta-doped samples, with \mathcal{R} values varying from 20 to 60. The "magneto-resistance mobility," μ_M , defined by

$$\rho(B) = \rho(0)(1 + \mu_M^2 B^2 + \dots),$$

is an effective mobility averaged over bands and crystalline directions.¹³ We have in fact found μ_M to be proportional to \mathcal{R} :

$$\mu_M = (6.5 \pm 0.7) \times 10^2 (\text{cm}^2/\text{V s}) \mathcal{R}.$$

Both the longitudinal and transverse resistivities saturate rapidly as T^{*3} .⁶ Therefore the uncondensed carriers are predominantly scattered by impurities at 4 K just as in conventional metals, and we expect the low-temperature mobility to be inversely proportional to the impurity concentrations c . The usual criterion for the validity of this relationship is $\epsilon_F \gg \hbar/\tau$. In NbSe₃ the application of this criterion is complicated by the many Fermi-surface (FS) sheets which survive the transitions. Nevertheless, focusing attention on the ellipsoidal electron pocket^{13,14} which contributes to the strongest SdH period, we find $\epsilon_F/(\hbar\tau^{-1}) \approx 900$ [using the known number of states within this pocket ($\sim 10^{18}\text{ cm}^{-3}$) and the observed mobility $270\,000\text{ cm}^2/\text{V s}$]. Since this pocket is the shallowest and the other sheets are even more degenerate, we feel justified in assuming

$$\mathcal{R}^{-1} \propto \mu_M^{-1} \propto c = c_0 + c_1. \quad (1)$$

In Eq. (1), c_1 is the Ta (or Ti) concentration which is controlled experimentally. The quantity c_0 is the residual concentration of defects and dislocations after all Ta impurities have been removed. In Fig. 1 (inset) a plot of \mathcal{R}^{-1} vs the nominal c_1 shows that c_0 is nonzero. We have attempted to reduce c_0 by annealing samples starting at 750 °C and cooling at a rate of 10 °C/h over several days. The annealed samples did not show noticeable improvements in \mathcal{R} or the measured characteristic field.

Silver paint was used to attach gold-wire probes to the sample in standard four-probe configuration. In all cases except sample 1 the sample was laid on a thin sapphire substrate which was thermally anchored to a copper substrate. Sample 1 was suspended by four wires inside a TO-5 can in a 500- μm He atmosphere. This mounting configuration which was more strain-free enabled sample 1 to be thermally cycled six times before damage was done to the contacts. In the pulsed non-Ohmic measurements, pulse widths of 5 to 100 μs were used with duty cycles varying from 10^{-5} to 10^{-3} . The problem with using very short pulses is that

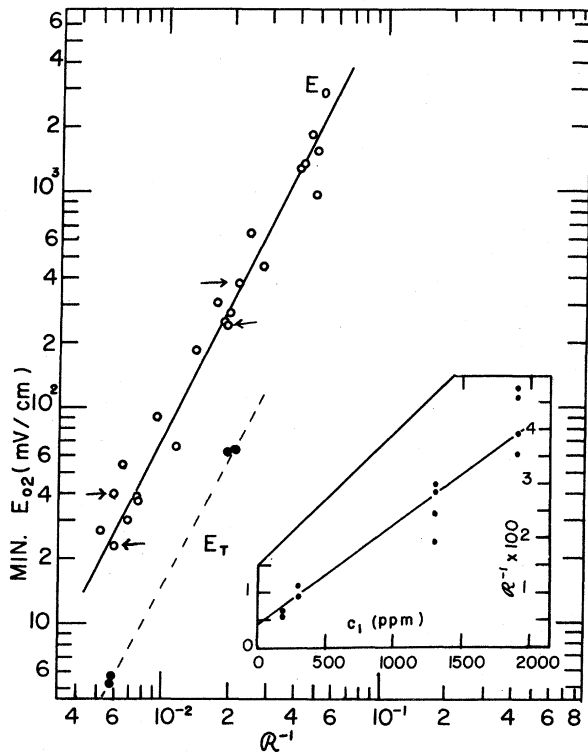


FIG. 1. Effect of Ta impurities on the characteristic field E_0 and threshold field E_T . Each open circle represents the minimum E_0 in a sample versus the reciprocal of the residual resistivity ratio \mathcal{R}^{-1} of the sample. The solid line has a slope of 2 implying the relationship $E_0 \sim \mathcal{R}^{-2}$. The minimum threshold field E_T (solid circles) also has a similar variation. In the inset the value of \mathcal{R}^{-1} is plotted versus the nominal concentration c of Ta impurities. The scatter represents the spread of \mathcal{R}^{-1} values in each crystal batch.

a new, hitherto unsuspected physical effect is being probed. We have found that this leads to a discrepancy between dc and pulsed results for *non-Ohmic* data at low applied fields for the pure samples. To avoid distortions due to this effect we have measured the onset of non-Ohmicity with a dc field. (For samples with $\alpha > 150$ self-heating is not a problem.) High-field results are obtained with pulsed voltage and agreement is established between the two methods at intermediate fields. In any case the low-field (Ohmic) value obtained by pulsed voltage is always checked against dc results. dc measurement of the Ohmic resistance is also performed before and after the non-Ohmic measurements (typically 45 min) to ensure that the temperature has not drifted or damage to the sample has not occurred.

Two methods were used to determine pulse heights. The first method of using an adjustable dc offset and monitoring the pulse shape on an oscilloscope was described in Ref. 2. In the second method the pulse height was measured directly by a dual-channel boxcar integrator (PAR 162/164). With the mainframe operating in the *A-B* mode one of the channels was used to subtract background fluctuations (mostly from 60-cycle pickup.) Gate aperture was kept at 1 μ s (0.1 pulse width) and the gate time constant was 1 ms. The voltage difference across the sample was converted to a single-ended signal by using an operational amplifier configured as a difference amplifier. The current through the sample was determined by measuring the voltage across a standard metal-film resistor in series with the sample and kept at room temperature. With sufficiently long integrating times the second method was reproducible to 3 parts in 10^3 for very small signals, and an order of magnitude more accurate than the first near the onset of non-Ohmicity. Only the data for sample 1 were taken with the boxcar.

In the microwave measurements the resistivity was obtained by the cavity perturbation technique.¹⁶ The change in the *Q* factor of the cavity was interpreted to be directly proportional to the resistivity of the samples (typically 4 mm \times 10 μ m \times 3 μ m) in accordance with the assumption that the absolute conductivity at all temperatures is not high enough to require a skin-depth regime analysis.¹⁷ The absolute value of the microwave conductivity at room temperature determined by using the depolarization equations¹⁶ agreed with the dc value to $\pm 10\%$. In our data we have normalized both sets of data so that they agree at all temperatures above the 142-K transition. The unloaded cavity *Q* was obtained by orienting the sample such that its needle axis is perpendicular to the rf electric field.¹⁸

III. RESULTS

NbSe₃ undergoes two CDW transitions at 142 K (T_1) and 58 K (T_2). Here we present data for the phase below the T_2 transition only. The early measurements by Ong and Monceau (OM) (Ref. 2) on the non-Ohmicity were fitted with the Zener-type expression

$$\sigma(E, T) = \sigma_a(T) + \sigma_b(T)e^{-E_0(T)/E}, \quad (2)$$

where E is the applied field and T the temperature. The first term σ_a is the Ohmic component of the conductivity. Because of the nonanalyticity of the σ_b term in the $E=0$ limit in Eq. (2), σ rises rapidly when non-Ohmicity sets in. Using dc derivative techniques FG (Ref. 8) found that the onset of non-Ohmicity is even more abrupt. They modified Eq. (2) by introducing a threshold field E_T as in the expression

$$\sigma(E, T) = \sigma_a(T) + \sigma_b(T)e^{-E_0(T)/[E - E_T(T)]}. \quad (3)$$

This has the effect of removing the slight downwards curvature evident in plots of $\ln(\sigma - \sigma_a)$ vs $1/E$ for low- E values (Figs. 3 and 4 in Refs. 1 and 2, respectively.)

As discussed in Ref. 2 the characteristic field E_0 is strongly temperature dependent. It attains a minimum approximately 10 K below the transition T_2 . For each sample we have chosen to compare E_0 at this minimum value with the residual resistivity ratio (α) in order to investigate the effect of Ta impurity concentration c on E_0 . Earlier results⁷ showed that E_0 varies as c^2 from a data base of 13 samples. Here we extend the data base to 22 samples and discuss the effect of introducing E_T .

A nonzero E_T has the effect of reducing the value of E_0 [the slope of the straight line obtained by plotting $\ln(\sigma - \sigma_a)$ vs $(E - E_T)^{-1}$] obtained from a least-squares fit to the data. However, at the temperature where E_0 and E_T are a minimum, E_T is very small and the reduction in E_0 is typically 20%. This is not significant compared to the data scatter in the log-log plot of E_0 vs α^{-1} in Fig. 1 of Ref. 7, which is reproduced here as Fig. 1 with new data inserted. The values of E_0 for four samples fitted to Eq. (3) (shown by arrows in Fig. 1) lie within the scatter of the plot. Thus the central result of Ref. 7 is left unaltered: The minimum characteristic field E_0 (and threshold field E_T) varies approximately as the square of the impurity concentration c . A least-squares fit gives an exponent of 1.90 for E_0 and 1.96 for E_T . The temperature dependence below 55 K of the non-Ohmic parameters E_0 , E_T , and σ_b were extensively studied in four samples. We found that the ratio E_0/E_T does not change appreciably with α . In the pure

samples E_0/E_T varies from ~ 5 to ~ 2.5 as the temperature decreases from 50 K. In dirtier samples E_0/E_T stays at approximately 3. Figures 2 and 3 show the conductivity σ vs E for a high-purity sample (no. 1) which has a value of α equal to 173. The solid lines are fits to the data using Eq. (3) at various temperatures. Figure 3 highlights the significant disagreement between the pulsed data and a fit based on Eq. (3) when the applied field is approximately 12 mV/cm. In the lower right of Fig. 3 this discrepancy is shown with the horizontal axis expanded by a factor of 10. Clearly the very abrupt jump in the pulsed

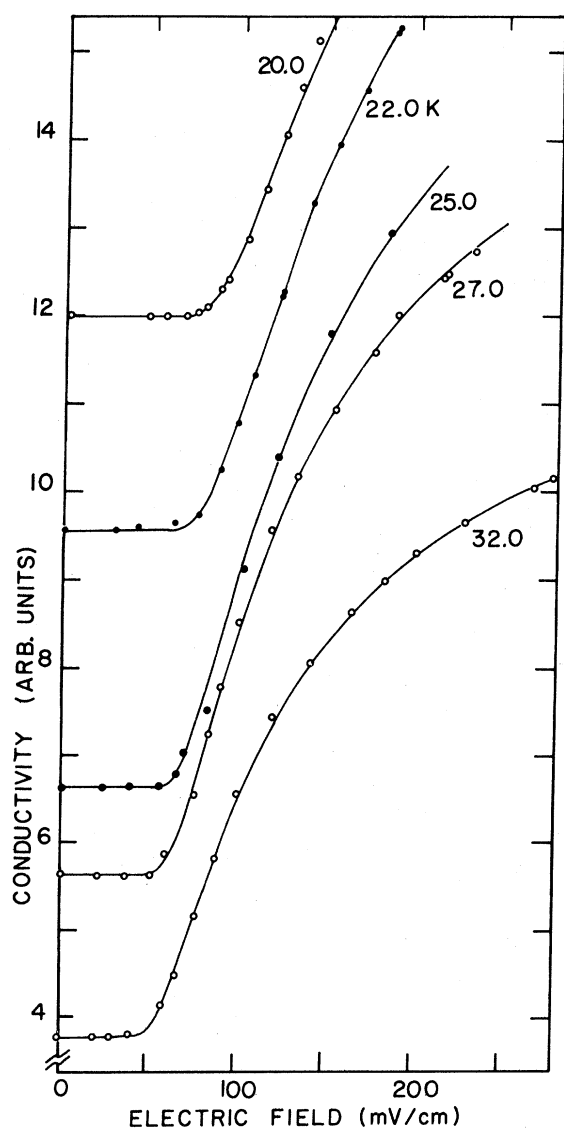


FIG. 2. Conductivity versus electric field at low temperatures for high-purity sample, sample 1 ($\alpha \sim 173$). The data were taken with pulses of width 14 μ s. Doublets in the data represent reproducibility checks. The solid lines are fits to Eq. (3).

conductivity (solid circles) at 52 K when the field exceeds 16 mV/cm cannot be accommodated by Eq. (3). In contrast the dc conductivity (open circles) can be fitted quite well with Eq. (3) (solid line). This discrepancy between the pulsed and dc data is an important physical effect intrinsic to the dynamical response of the CDW condensate and is being further pursued. We have ruled out extrinsic causes such as the time constants of electronic components. A preliminary report is presented elsewhere.¹¹

Figure 4 shows a linear-scale plot of data from a 1300-ppm Ta sample (no. 2) with $\alpha = 53.0$. The temperature dependence of the non-Ohmic parameters can be extracted from the fits in Figs. 2, 3, and 4. In this paper we focus on the temperature dependence of these parameters below 50 K. For sample 1 these are displayed in Fig. 5. Compared to the early results of OM (Ref. 2) on pure samples the effect of E_T is to round off the sharp minimum in E_0 as a function of T . Both E_0 and E_T attain a minimum near 50 K. More significantly, α defined as $\sigma_b/(\sigma_a + \sigma_b)$ decreases with temperature after attaining a maximum at 36 K. Previous fits⁸ with $E_T = 0$ had indicated that α saturates and remains temperature independent below 36 K. The new evidence for a decreasing α appears to be quite strong. A plot of $\ln[(\sigma/\sigma_a) - 1]$ vs $(E - E_T)^{-1}$ shows that the y -axis intercept which is equal to $\ln[(\sigma_b/\sigma_a) - 1]$ clearly decreases with temperature below 36 K. As such the original interpretation by OM of α as a measure of the fraction of FS affected by the CDW gap is now untenable. [This interpretation also relies on the further assumption that in the limit of infinite field the pretransition conductivity (adjusted for phonon effects) is exactly recovered. For future discussion we shall refer to this assumption as the infinite-field conductivity hypothesis.] Figure 6 shows the non-Ohmic parameters for sample 2 ($\alpha = 53$). As mentioned before, E_0/E_T is less temperature dependent in dirtier samples.

The non-Ohmicity in samples doped with Ti has also been studied. Since Ti is a group-IV impurity it is not isoelectronic with Nb and exists as a charged impurity. Thus, it is expected to interact with the CDW condensate more strongly. Experimentally we find that the introduction of Ti has a more pronounced effect on E_0 and α than the case with Ta. For a nominal c of 1000-ppm Ti the values of α cluster around 2 (compared to 50 for 1000-ppm Ta). No non-Ohmic effect⁷ is observed up to fields of 6 V/cm. (The threshold field is 60 mV/cm for 1000-ppm Ta samples.) For a second batch of 100-ppm Ti samples, α varied from 4 to 29. The measured $E_{0\min}$ varied from 3 to 0.35 V/cm (compared with 30 mV/cm for typical 180-

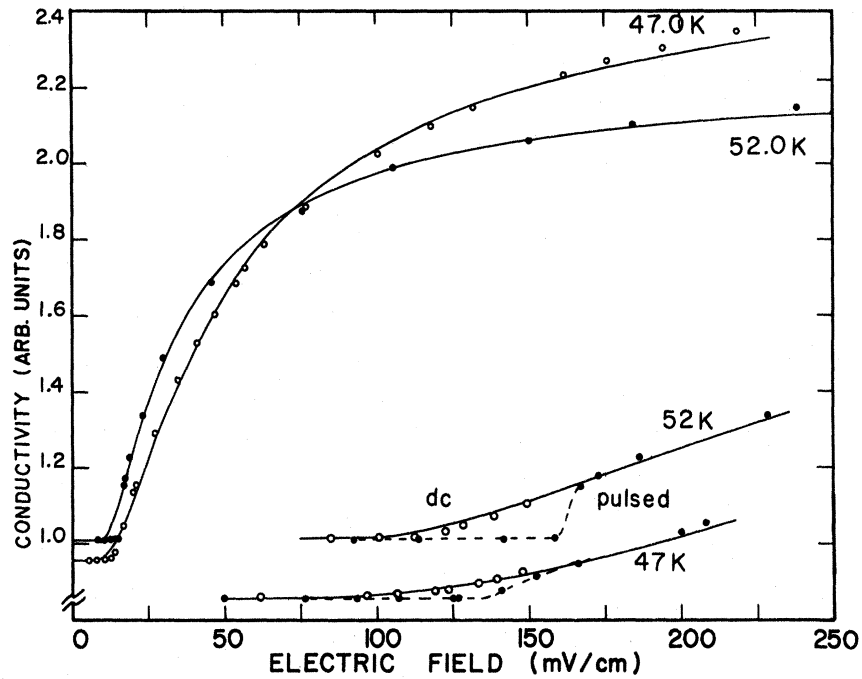


FIG. 3. Conductivity versus electric field for sample 1 showing discrepancy between pulsed and dc data very near threshold. Solid lines are fits to Eq. (3). In the lower right of the figure the horizontal axis has been expanded by a factor of 10. Here, the open circles represent dc measurements while solid circles are obtained with pulses of width $2 \mu\text{s}$. The broken lines are drawn as a guide to the eye. The discrepancy is ascribed to transient effects due to the depinning of the CDW condensate.

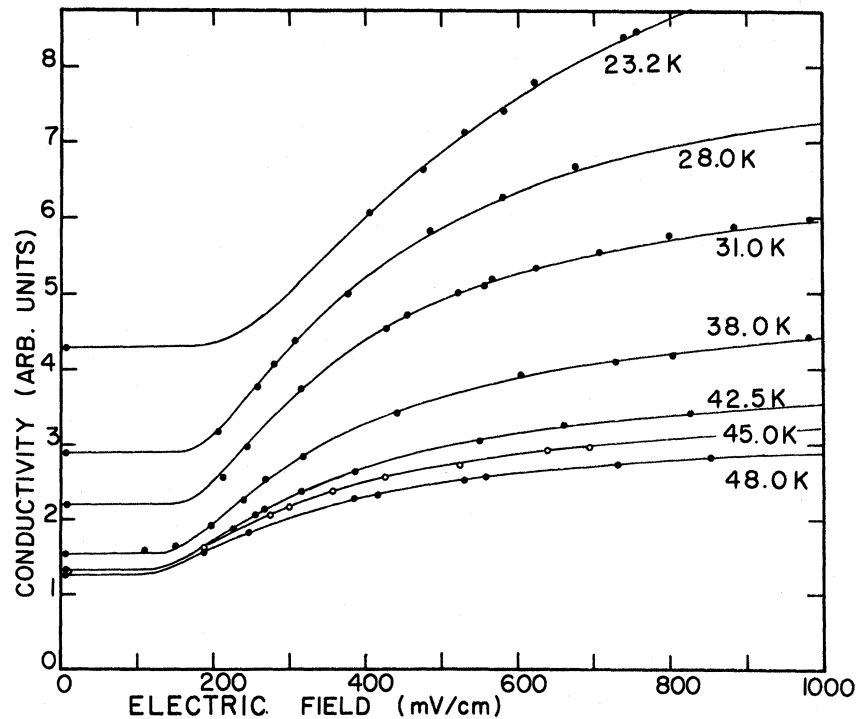


FIG. 4. Conductivity versus electric field for a moderate-purity sample, no. 2 ($\theta \sim 53$). The measurements were carried out with pulses of width $14 \mu\text{s}$.

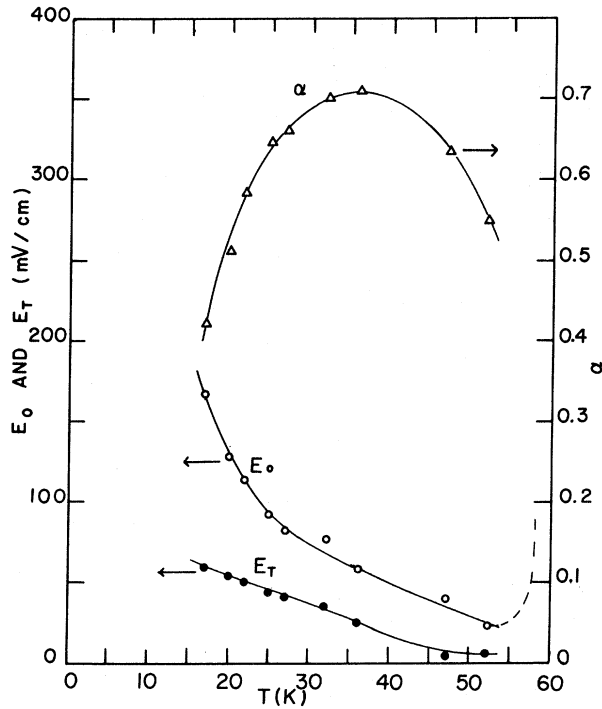


FIG. 5. Non-Ohmic parameters α , E_0 , and E_T versus temperature for sample 1. Unlike previously reported data, α is nonmonotonic. All lines are eye-guides. The broken line for E_0 above 50 K indicates behavior near T_2 .

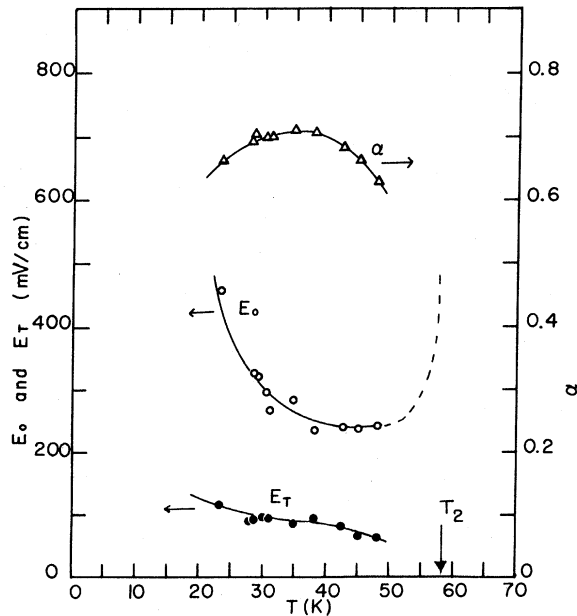


FIG. 6. Non-Ohmic parameters α , E_0 , and E_T versus temperature for sample 2. The broken line for E_0 above 50 K indicates behavior near T_2 .

ppm Ta samples). No smooth variation of $E_{0\min}$ with α comparable to the Ta case was obtained with the 8 Ti-doped samples investigated. This may be due to the difficulty in controlling homogeneity in our doping process (with Ti) and the strongly disruptive effect Ti has on the host lattice. For some 1000-ppm Ti samples, the (Ohmic) dc resistivity below the T_2 transition rises monotonically with decreasing temperature (see Fig. 8) instead of resuming metallic behavior below 40 K as in comparably doped Ta samples. This interesting behavior is not understood in terms of the canonical FS gapping picture. Similar monotonic increase in the dc resistivity has also been observed in neutron-irradiated samples (W. Fuller and P. Chaikin, private communication).

The dramatic effect of impurities on the excess microwave absorption is shown in Figs. 7 (Ta impurities). In both figures data points refer to 9.8-GHz results while solid lines are dc Ohmic results on the same sample. The 300-ppm Ta sample (*D* in Fig. 7) shows a large discrepancy between the dc and 9.8-GHz resistivities similar to the nominally pure case reported in Ref. 2. [It is important to distinguish this discrepancy from the dc non-Ohmic effect which produces a superficially similar curve at very high electric fields (see Ref. 1)]. In all the microwave measurements the power incident on the cavity was kept under a few microwatts. The reduction in Q was consistent with electric fields smaller than threshold inside the sample (taking into account the depolarizing effect). Thus the 9.8-GHz data here refer to the high-frequency Ohmic regime. Referring to the discrepancy between the dc and microwave data as the excess microwave absorption we see that as the Ta content increases (*D* to *C* to *B*) the excess absorption decreases. When the impurity concentration is approximately 5000 ppm (*B*) the excess absorption is almost completely suppressed in the T_1 phase. A similar suppression of the excess microwave absorption is seen in Fig. 8 for Ti impurities. At the higher concentration (1000 ppm) no excess absorption is seen down to 30 K. For the 100-ppm sample, excess absorption is evident at all temperatures below T_1 .

Two qualitative features are worth emphasizing here. First, whereas a 1000-ppm concentration of Ti is sufficient to remove almost all the excess conductivity, a similar concentration of Ta impurities (corresponding to a case intermediate between *C* and *D* in Fig. 7) affects the excess conductivity only slightly. Hence Ti is much more effective than Ta in suppressing the anomalous microwave response. Secondly, comparing samples *C* and *D* we see that increasing the Ta content from 300 to 1900 ppm hardly affects the excess conduc-

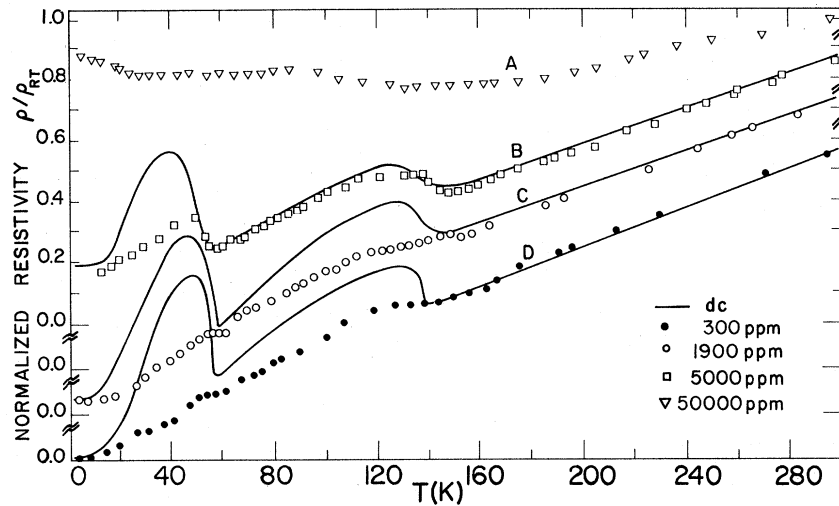


FIG. 7. Resistivity at 9.8 GHz for four samples of different Ta concentration. Solid lines are dc measurements of the linear resistivity in the same samples. The discrepancy between dc and the 9.8-GHz values (the "excess absorption") represents the excess ac conductivity due to the forced oscillation of the pinned condensate. This excess absorption is suppressed with increasing Ta concentration.

tivity at 9.8 GHz. However, the effect on the dc non-Ohmicity is quite pronounced. The data in Fig. 1 show that E_0 increases from 50 mV/cm (for $\mathcal{R} \sim 18$). A discussion of these results is given in Sec. V.

IV. GOODNESS OF FIT

At each temperature the fit to the dc non-Ohmic data has three adjustable parameters σ_b , E_0 , and

E_T . (σ_4 is fixed by dc measurement.) The least-squares method we used is to minimize the reduced chi-squared. As shown in Fig. 2 the proposed fit of FG can describe the non-Ohmic data very well up to field values corresponding to a two-fold increase in σ . For higher values of E the fit is less satisfactory (see Fig. 3, 47 K) and the minimization procedure produces a fit which succes-

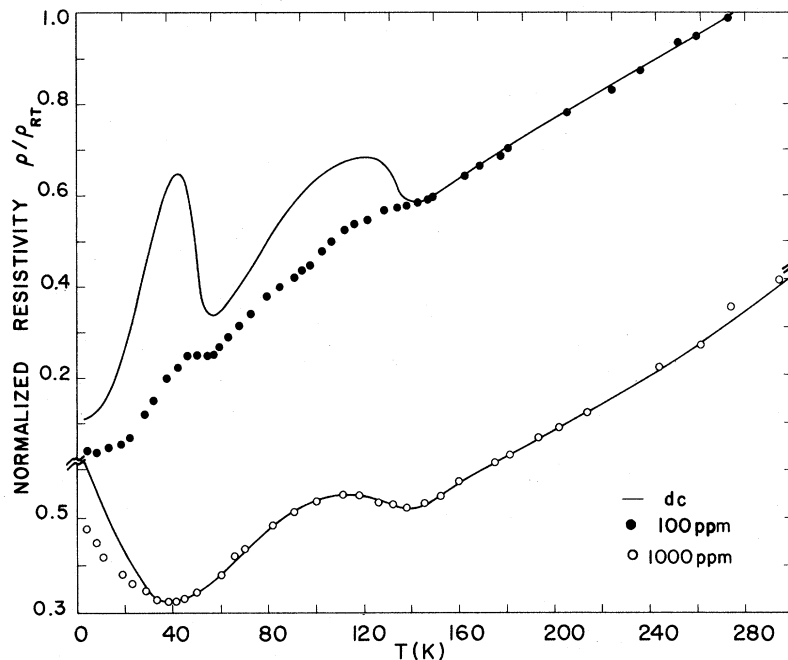


FIG. 8. 9.8-GHz resistivity of Ti-doped samples compared with the dc resistivity (solid lines).

sively overshoots and undershoots. In fact, the similarity in the behavior of E_0 and E_T as a function of temperature and impurity concentration suggests that Eq. (3) is quite possibly a three-parameter fit to the true function. Nonetheless it is a highly accurate approximation and serves to summarize the T and c dependence of the non-Ohmicity in a convenient way. The correct model presumably will produce a non-Ohmic function which mimics Eq. (3) and be an even better fit to the data.

With this caveat we now discuss the recent measurements on the non-Ohmic conductivity of NbSe₃ by Gill⁹ and by Richards and Monceau (RM).¹⁰ Gill presented extensive pulsed voltage data both in the T_1 phase and the T_2 phase. In the T_1 phase Gill found that Eq. (3) is obeyed with the non-Ohmic parameters varying smoothly with temperature. However, below T_2 Gill uses two σ_b terms to describe the non-Ohmicity, corresponding to the two CDW's. Between 51 and 31 K Gill's data plotted in log-log scale show a nonmonotonic second derivative for low fields. This variation is interpreted as the two CDW's locking in to each other. Below 31 K the two CDW's move together and Gill reverts to one non-Ohmic term which he labels by subscript 3. Although the general trend of his non-Ohmic parameters are roughly in agreement with the data in this paper and previously published results,² we do not see any evidence for the lock-in transition between 31 and 51 K. Our data plotted in log-log scale do not show nonmonotonic behavior in the second derivative at any temperature below T_2 . In all samples studied the temperature variation of the non-Ohmic parameters as well as the field dependence of σ at fixed temperature do not support Gill's model.

In a tour de force study RM have amassed extensive data on both the temperature and pressure dependence of the non-Ohmic parameters in a single sample with $\alpha=38$ below T_2 . High-field data (up to 8 V/cm) show that the onset of non-Ohmicity due to the T_1 -CDW is clearly seen. Unfortunately, RM find that Eq. (3) gives a poor fit to their low-field data and choose to characterize their results by a new parameter, the critical field E_{c2} , at which non-Ohmicity associated with the T_2 -CDW first appears. We suggest the possibility that the low-field disagreement from Eq. (3) may be due to the very short pulse widths used. This will result in a more abrupt rise of the conductivity compared with the dc data as we have shown in Fig. 2 for 47 and 52 K. If this is the case then Eq. (3) is not in fact applicable when $(\sigma/\sigma_a - 1)$ is very small. Furthermore, E_{c2} is a pulse-width-dependent parameter and is not an unambiguous quantity unless the pulse width is also specified.

V. DISCUSSION OF RESULTS

The central experimental finding here is that the characteristic field E_0 (and less firmly E_T as well) varies as c^2 over two orders of magnitude when NbSe₃ is doped with Ta impurities on the non-Ohmicity in NbSe₃.

The most complete model is that of Lee and Rice⁵ (LR). Building on the original idea of Fröhlich,³ LR ascribe the non-Ohmicity to the depinning of the charged CDW condensate from the underlying host lattice. We reproduce LR's argument here in a more pedestrian (and hopefully more transparent) fashion. There are two classes of impurities. In the strong-impurity pinning case the CDW gains enough energy from each impurity site to overcome the local strain energy cost in achieving the minimum energy configuration. Thus the CDW distorts its phase and amplitude to accommodate each impurity. In the weak-impurity pinning case (presumably the case with Ta) the gain per impurity is never sufficient to compensate for local distortions. However, the CDW can still gain energy from a large collection of weak impurities by breaking up into three-dimensional domains of length L . Within each domain the phase and amplitude are uniform, with the phase adjusting itself to optimize the gain in energy from the impurities. LR's arguments (also Fukayama and Lee¹⁹) may be simplified as follows (ignoring anisotropy for simplicity). The gain in free energy from the impurities within each domain is

$$\Delta F_{\text{pin}} = -V_{\text{imp}}\rho \sum_i e^{i(\vec{Q}\cdot\vec{x}_i+\phi)} = -V_{\text{imp}}\rho e^{i\bar{\phi}} \sum_i e^{i\vec{Q}\cdot\vec{x}_i},$$

where V_{imp} is the impurity potential, ρ is the CDW charge density, \vec{Q} is the CDW spanning vector, and \vec{x}_i are the impurity sites. The sum is confined to sites within a domain and $\bar{\phi}$ is the optimum phase. Since \vec{x}_i is random the sum is just equal to the random walk result, i.e., the square root of the number of terms in the sum. Therefore the free energy gained per unit volume is

$$\frac{\Delta F}{L^3} = -V_{\text{imp}}\frac{\rho}{L^3}(cL^3)^{1/2} = -V_{\text{imp}}\frac{\rho\sqrt{c}}{L^{3/2}}. \quad (4)$$

The cost in free energy per unit volume is mainly from the elastic strain term

$$\frac{\Delta F}{L^3} = f \int \frac{\xi^2 |\nabla\psi|^2 d^3x}{L^3} \approx f\xi^2 \frac{|\psi|^2}{L^2}, \quad (5)$$

where ξ is the coherence length and ψ the order parameter. Minimizing the sum of Eqs. (4) and (5), we find that the optimum length is

$$L_0 = (\frac{4}{3}f\xi |\psi|^2 / V_{\text{imp}}\rho)^{2/3} / c. \quad (6)$$

With this optimum length the net free energy den-

sity gain is found to be $-\frac{1}{3}f\xi^2|\psi|^2/L_0^2$. For an electric field E to dislodge the CDW condensate over one wavelength $2\pi/Q$, it has to supply enough energy to overcome this net pinning energy. Thus

$$\rho E \left(\frac{2\pi}{Q} \right) \simeq \frac{1}{3}f\xi^2|\psi|^2/L_0^2. \quad (7)$$

From Eqs. (6) and (7) we have that the characteristic field varies as the square of the impurity concentration c . Furthermore, because ρ represents a macroscopic charge density the required E field can be quite small. To be sure, the above picture is oversimplified. For one thing conversion between the free carriers and the condensate is always occurring in the drifting situation (at the domain walls, for instance), as well as exchange of momentum. As a result the free carriers and the drifting condensate are strongly coupled. (This has been advanced⁵ by LR as a possible reason for the conductivity saturation at "infinite" fields.) Nonetheless, it is remarkable that Eq. (7) anticipates the experimental result on c . The functional form of the non-Ohmic conductivity [Eq. (3)] is not addressed by LR, nor the temperature dependence of E_0 and E_T .

In Bardeen's model²⁰ motion of the rigid CDW is achieved by tunneling of the whole CDW across gaps E_g induced by the pinning potential (either from impurities or superlattice commensurability). Arguing that these minigaps are of the order of $\hbar\omega_p$ (the pinning frequency) Bardeen arrives at a non-Ohmic conductivity of the form in Eq. (2) with

$$E_0 = \pi(\hbar\omega_p)^2/(4\hbar e^* v_F), \quad (8)$$

where e^* is an effective charge and v_F is the electron Fermi velocity. Equation (8) gives the right order of magnitude for E_0 if ω_p is assumed to be 9 GHz. Bardeen suggest²⁰ that E_0 should also vary as c^2 if the pinning frequency increases as c . An experimental investigation of the impurity effect on the frequency dependence of σ is clearly of great interest.

Maki²¹ has explored soliton models in which the applied field leads to pair creation of solitons in a strictly one-dimensional CDW or to a nucleation and growth of two-dimensional domains. These models also reproduce Eq. (2) but the effect of impurities has not been incorporated into his calculations.

We now briefly discuss the new observation that the onset of non-Ohmicity depends on the width of the pulse used (see Fig. 2 data for 47 and 52 K). Figure 3 shows that as the pulse width is decreased from dc (milliseconds) to 1 μ s the onset of non-Ohmicity is postponed to larger fields. For very short pulses the onset may be very abrupt (see 52

K data, solid circles). This unexpected behavior is due to the transient response of the condensate to a step voltage. We tentatively identify the delay in observing the onset of non-Ohmicity (when the pulse width is very short) as a manifestation of the inertia of the Fröhlich mass. Thus if the conductivity is sampled too soon after the leading edge of the step voltage the massive condensate fails to contribute to the conductivity, even if E exceeds E_T .

Portis²² has recently proposed that the exponential dependence of the non-Ohmic dc conductivity may be accounted for by a Poisson distribution of pinning strengths. As the electric field increases an increasing number of chains (or domains) slip. There is experimental support for such a distribution from recent measurements on the frequency dependence of the linear conductivity by Longcor and Portis²² and Grüner *et al.*²³ Portis's model is phenomenological and does not address the impurity dependence of the non-Ohmicity or the temperature dependence of the non-Ohmic parameters. However, it does suggest a natural way to explain the exponential increase in conductivity within the sliding Fröhlich model.

The frequency dependence results obtained by Grüner *et al.*²³ between 15 and 250 MHz on pure samples are helpful in interpreting the microwave results presented here. Instead of a Lorentzian spectrum, the measured spectrum resembles a highly damped oscillator in which the damping term dominates the inertial term. Longcor and Portis²² have modeled the spectrum with an RC series combination in parallel with a second resistor R_2 which represents the conduction channel of the uncondensed electrons. At frequencies smaller than $(RC)^{-1}$ the conductance is due to the free carriers ($\sim R_2^{-1}$). At frequencies above $(RC)^{-1}$ the impedance of the capacitance is negligible and the conductance increases to the parallel combination value $(R + R_2)/R R_2$. Presumably the microwave measurements are all in the high-frequency limit which has little frequency dependence (because the capacitance impedance becomes insignificant). This explains why the curves C and D in Fig. 7 are similar despite a factor of 6 increase in Ta concentration c . Nonetheless the introduction of more impurities eventually shifts the crossover frequency $(RC)^{-1}$ to microwave frequencies as may be seen in curve B ($c = 5000$ ppm). At this level of impurities at 9.8 GHz the T_1 phase is now in the low-frequency region while the T_2 phase is right in the crossover region. Grüner *et al.*'s data show that $(RC)^{-1}$ is 60 MHz for a pure sample (300-ppm Ta) at 42 K while the data here show that $(RC)^{-1}$ is 9.8 GHz at the same temperature for the 5000-ppm sample. Thus the increase in $(RC)^{-1}$ is 10

times larger than the increase in impurity concentration (170 vs 17). Defining parameters by the harmonic oscillator equation

$$M_{\text{CDW}}(\ddot{x} + \Gamma\dot{x} + \omega_0^2 x) = F, \quad (9)$$

we see that $(RC)^{-1} = \omega_0^2/\Gamma$. Thus the rapid increase in $(RC)^{-1}$ is due to both an increase in ω_0 and a drastic decrease in Γ (inverse lifetime). To get a more complete picture we need to add an inductor in series with RC in the Longcor-Portis circuit. At sufficiently high frequencies (perhaps in the submillimeter region) the conductivity decreases to the zero-frequency value because of the choke effect of the inductor. This high-frequency crossover (the "Drude" edge of the *pinned* condensate) is easily seen to occur at Γ . Such a measurement would be very illuminating and in effect would determine all the parameters in Eq. (9).

ACKNOWLEDGMENTS

Illuminating discussions with J. Bardeen, P. M. Chaikin, R. M. Fleming, W. G. Clark, P. A. Lee, K. Maki, P. Monceau, A. M. Portis, and T. M. Rice are gratefully acknowledged. We thank R. M. Fleming, P. Monceau, J. Bardeen, S. Longcor, P. A. Lee, and T. M. Rice for sending manuscripts prior to publication. The help of Y. R. Lin-Liu in the data analysis has been indispensable. Part of this work represents one phase of research performed by the Jet Propulsion Laboratory and the California Institute of Technology, sponsored by the National Aeronautics and Space Administration, Contract No. NAS7-100. Work at U.S.C. was jointly sponsored by the U.S. Office of Naval Research, Contract No. N00014-77-C0473, and by the National Science Foundation, Contract No. DMR-7905418.

*Present address: Department of Physics and Astronomy, University of Kentucky, Lexington, KY 40506.

¹P. Monceau, N. P. Ong, A. M. Portis, A. Meerschaut, and J. Rouxel, *Phys. Rev. Lett.* **37**, 602 (1976).

²N. P. Ong and P. Monceau, *Phys. Rev. B* **16**, 3443 (1977).

³H. Fröhlich, *Proc. R. Soc. London Ser. A* **223**, 296 (1954).

⁴D. Allender, J. W. Bray, and J. Bardeen, *Phys. Rev. B* **9**, 119 (1974).

⁵P. A. Lee and T. M. Rice, *Phys. Rev. B* **19**, 3970 (1979).

⁶R. M. Fleming, D. E. Moncton, and D. B. McWhan, *Phys. Rev. B* **18**, 5560 (1978).

⁷N. P. Ong, J. W. Brill, J. C. Eckert, J. W. Savage, S. K. Khanna, and R. B. Somoano, *Phys. Rev. Lett.* **42**, 811 (1979).

⁸R. M. Fleming and C. C. Grimes, *Phys. Rev. Lett.* **42**, 1423 (1979).

⁹J. C. Gill, *J. Phys. F* **10**, L81 (1980).

¹⁰J. Richard and P. Monceau, *Solid State Commun.* **33**, 635 (1980).

¹¹N. P. Ong and G. X. Tessema, *Bull. Am. Phys. Soc.*

25, 341 (1980).

¹²A. Meerschaut and J. Rouxel, *J. Less-Common Met.* **39**, 197 (1975).

¹³N. P. Ong, *Phys. Rev. B* **18**, 5272 (1978).

¹⁴P. Monceau and A. Briggs, *J. Phys. C* **11**, L465 (1978).

¹⁵N. P. Ong and J. W. Brill, *Phys. Rev. B* **18**, 5265 (1978).

¹⁶L. I. Buranov and J. F. Shchegolev, *Prib. Tekh. Eksp.* **2**, 171 (1971).

¹⁷M. Cohen, S. K. Khanna, W. J. Gunning, A. F. Garito, and A. J. Heeger, *Solid State Commun.* **17**, 367 (1975).

¹⁸S. K. Khanna, E. Ehrenfreund, A. F. Garito, and A. J. Heeger, *Phys. Rev. B* **10**, 2205 (1974).

¹⁹H. Fukuyama and P. A. Lee, *Phys. Rev. B* **17**, 535 (1978).

²⁰J. Bardeen, *Phys. Rev. Lett.* **42**, 1498 (1979).

²¹K. Maki, *Phys. Rev. Lett.* **39**, 46 (1977), *Phys. Lett.* **70A**, 449 (1979).

²²S. W. Longcor and A. M. Portis, *Bull. Am. Phys. Soc.* **25**, 340 (1980).

²³G. Grüner, L. C. Tippie, J. Sanny, W. G. Clark, and N. P. Ong, *Phys. Rev. Lett.* **45**, 935 (1980).